IET Generation, Transmission & Distribution

Research Article

ISSN 1751-8687
Received on 20th July 2019
Revised 9th September 2019
Accepted on 13th January 2020
E-First on 14th February 2020
doi: 10.1049/iet-gtd.2019.1118
www.ietdl.org

On-line monitoring device for dry zone formation in the soil surrounding underground power cables

Osama E. Gouda[1] ✉, *Gomaa F.A. Osman*[2]
[1]*Faculty of Engineering, Cairo University, Egypt*
[2]*Benha Faculty of Engineering, Benha University, Egypt*
✉ *E-mail: prof_ossama11@yahoo.com*

Abstract: Formation of dry zones around power cables is an important factor affecting the cable loading and may lead to cable failure. This phenomenon is ignored by some standards in the calculation of power cables capacity. Numerous efforts have been done by many researchers for cable monitoring. In this study, monitoring system based on measurements of temperature distribution surrounding the cable route is suggested. When reaching the temperature of the dry zone formation the system will produce a warning alarm. To the best of the authors knowledge, the invention of a device that gives a warning in the case of drying layers formation around the power cables has not received attention so far. The proposed device is characterised by cheap price, high accuracy and its simplicity in the design. The system is tested in the laboratory using different soil types. Field tests are done to verify the reliability of the device.

1 Introduction

As it is known the losses of power cables produce heat increases the cable temperature. The thermal stability around the cable is necessary to keep the cable conductor and insulation temperatures within the allowable limits [1–4]. Because of the soil temperature increase, the surrounding back-fill soils around underground power cables lose their moisture content, forming dry areas [5–10]. This leads to an increase in the soil thermal resistance and decreases the maximum current carrying capacity of the underground power cables.

Soil thermal resistivity is affected mainly by soil composition, degree of compaction, dry density, gradation, water content and temperature rise [1–10]. The problem of coupled heat and water flows around buried cables was investigated by several authors [11–20]. Numerical simulation to study the heat dissipation processes in the underground power cable, thermal analysis of power cables are investigated by the authors of [11, 12, 19]. Theoretical models to calculate steady-state, dynamic ampacity and emergency current ratings of underground power cables are discussed in [20–27].

After the long operation of power cables for several years, dried out zones are usually formed around the cables. These zones may lead to thermal instability of the soil surrounding the cables. Consequently, the ability of the soil to dissipate the heat is much decreased and finally thermal cable failure may happen experimental study for drying-out formation is done in [28–38]. The maximum current carrying capacity of a buried power cable depends on the heat produced by cable losses, insulation layers thermal resistances and the thermal characteristic of the soil surrounding the cables. The formation of a dry zone leads to a marked decrease in the cable current rating by about 29% of its rating when the dry out occurs [34]. For safe operation of buried cables, bedding soils are used to reduce soil thermal resistivity and to minimise moisture migration [34]. To eliminate the dry zone formation and to maximise the heat transfer and increasing the cable capacity the back-fill soil around the cable should be graded, having higher ratios of loam content and be compacted at optimum water content for maximum dry density [34].

A real-time software system taking inputs from the power cables by using temperature sensor is used as a technique for monitoring the cable safe operation based on Electra 87 as recommended in IEC60287 and IEC60853. Janda *et al.* [39] recorded the critical temperature of dry area formation around high voltage cable systems by using a set of elements, which are installed at hot spots of the power cable route and in the substation. The communication between the measurement spot and substation was carried out using an optical cable system. Singh [40] used the same technique of monitoring system taking inputs from the power distributed temperature sensor. IEC60287 presented a formula to calculate the current ratings of underground power cables as a function of the cable properties and surrounding soil characteristics and it is modified to comply with dry band formation [1].

The aim of this paper is to propose a device for monitoring the dry zone formation around the cable. The proposed monitor is characterised by cheap price comparing with other systems, good accuracy in monitoring and its simplicity in the design. The monitor is tested in the laboratory using different soil types and it gave good monitoring for dry zone formation in the back-fill soil. It is tested also in the field and the device has demonstrated accuracy in the definition of the dry zone around the cable path at the site. Its accuracy reached to about 98.3% after 60 tests done in the laboratory and 98.5% after about 150 tests done in the field. Finally, it is on-line monitor, so there is no time consuming.

2 Monitoring device construction and operation

The suggested dry zone indication device is constructed as shown in Fig. 1*a*. The main components of this device are a reference voltage control unit, signal conditioning circuits, comparator circuits, isolation circuits, and output alarm device. Fig. 1*b* gives the details of the signal conditioning and comparator circuits.

The function of each element of the device can be explained as follows:

i. The system is provided with a group of temperature sensors (thermocouples) each one gives output voltage in mV represents the soil temperature. Each thermocouple voltage is then amplified and used as input to the device for monitoring the temperature rise. The amplifying circuit characteristic is as given in (1)

$$V_1 = V_{\text{in}}(1 + A) \quad (1)$$

where V_{in} is the thermocouple output voltage, V_1 is the output voltage of the amplifying circuit and A is the gain of the amplifying circuit.

ii. Reference voltage control unit is used to control the quantity of reference DC voltage input to the comparator circuit; this reference voltage is related to the level of dry zone formation temperature and is changed depending on the critical temperature (the temperature at which the dry zone is formed) of the soil type around the underground power cables.

iii. The signal conditioning circuit is used for processing, amplifying and filtering the output signal of the thermocouple sensor to be appropriate for the next operating step.

iv. The comparator circuit is used to compare the amplifying signal obtained by the previous stage with the external reference DC voltage; this DC voltage is controlled to be equivalent to the dry zone temperature of the cable surrounding soil. When the signal given from the conditioning circuit is higher than the adjusted reference DC voltage of the comparator an alarm output signal to operators will be sent by the device.

The comparator circuit operations are defined by the following equations:

$$\begin{aligned} &\text{If } V_1 \geq V_{\text{ref}} \text{ then } V_o = V_{cc} \\ &\text{If } V_1 < V_{\text{ref}} \text{ then } V_o = 0 \end{aligned} \quad (2)$$

where V_{ref} is the reference DC voltage, V_o is the output voltage of the comparator circuit and V_{cc} is the common voltage of the op-amp.

v. The isolation circuit consists of the transistor and output relay. It is used to isolate the low voltage, current signal conditioning and comparator circuits from one side and the voltage and current of the alarm device circuit from the other side.

vi. The output alarm device is used to send an alarm signal when the device senses the temperature of the dry band formation around the underground power cables.

The flowchart of the soil dry zone testing system operation steps are summarised in Fig. 2.

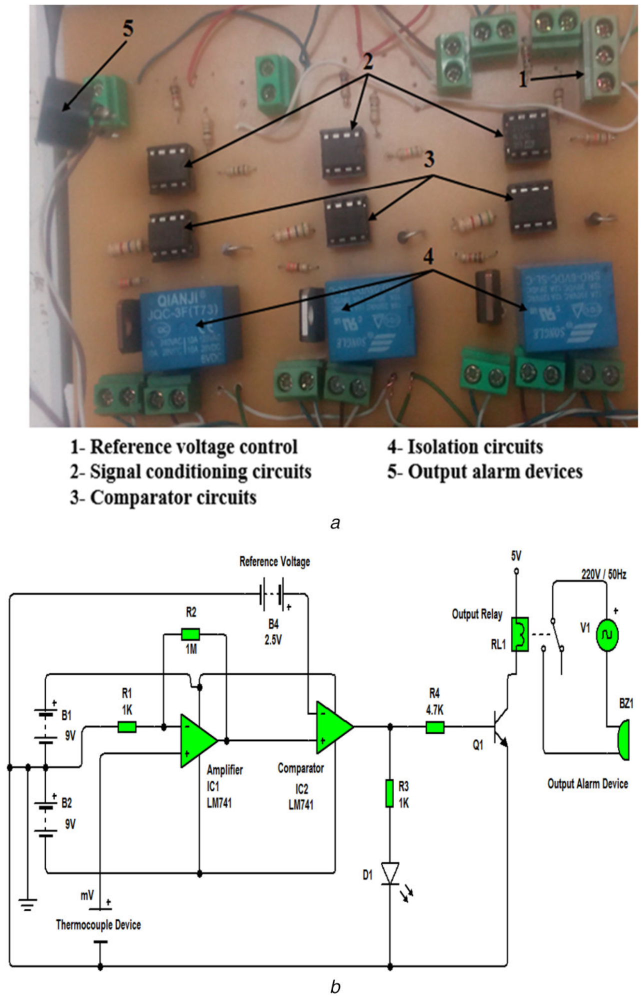

Fig. 1 *Soil dry zone indication device*
(a) The device elements,
(b) Signal conditioning and comparator circuits

3 Soil characteristic used in testing of the suggested device

3.1 Soil samples used in the test as back-fill material

A study has been carried out on a group of soil that can be used as back-fill materials around the underground power cables which differ in their components and moisture content as given in Table 1. As noted in this table, the amount of sand differed from 87 to 15%, and in contrast, the quantities of clay have ranged between 10 and 83%. The moisture content has been changed from 3.2 to 20%.

3.2 Arrangement of the soil performance testing

Fig. 3 shows the arrangement sketch that is used to study the different soil samples characteristics which can be used as back-fill materials for power cables. Each tested sample is placed in a cylindrical plastic container with a 10 cm diameter. The soil sample height was 10 cm. In the plastic container top part, a heater of known power to simulate the cable losses is inserted. The heat flux is measured by means of a calibrated heat flux meter. The power to the heater is controlled by means of auto-transformer which is connected from the primary side to the 220 V supply.

The sample bottom is in contact with a porous slab of sintered Pyrex glass with small pores diameter of 5 mm. A vessel of plastic completely filled with water that is provided with a flexible tube is used to simulate the groundwater table artificially. The cylinder containing the soil sample under testing has been sealed off by O-rings against the top wall of the insulated level. By this arrangement, the moisture tension and thus water content can be adjusted. A number of thermo-couples are placed with the walls at the axis of the sample that provide a possibility of measuring the temperature distribution at different points of the tested soil sample.

3.3 Results of the soil performance tests

Each soil sample is heated by using the heater element as given in Fig. 3 which is controlled to produce heat flux density 650 W/m^2. The tests are done at infinity suction tension. The suction tension affects the thermal soil resistivity and the temperature and the time of the dry zone formation around the underground power cables. The retention of soil moisture is described by the moisture potential (α) which is known as the suction tension of the soil in a water column and is usually expressed by the following relation:

$$Pf = \log(-100\ \alpha) \quad (3)$$

In (3) Pf is the suction tension and (α) is the moisture potential. For practical applications, the suction tension depends mainly on the soil moisture content, and the soil history of drying and wetting. In general, the Pf value in winter can be considered as 2 and less and in summer its value can be considered higher than 2.

The grain size of the selected soil samples under testing was ranged between 0.15 and 1.18 mm. During soil testing, the average total porosity measured value was 21.1%. The soil thermal characteristics of the tested soil are given in Table 2. From this table, it is noticed that the required time for the start of dry band formation increases with the clay percentage increase. This can be understandable because the clay retains moisture for a longer time than sand. Each tested soil sample wet thermal resistivity, dry thermal resistivity at starting and at the end of dry zone formation, its critical temperature and time to be formed are given in Table 2.

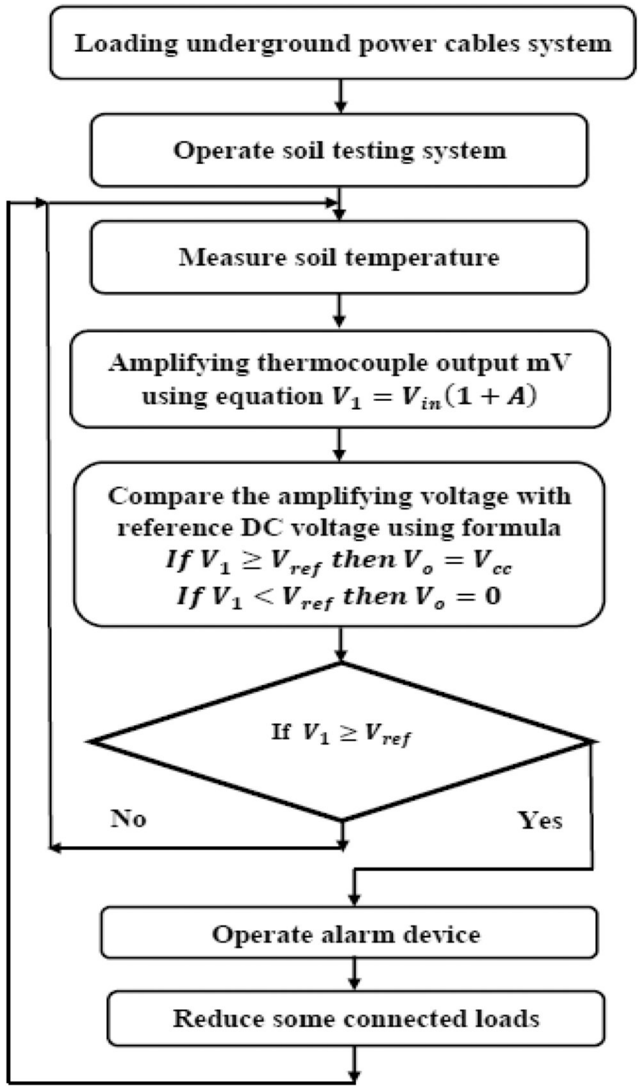

Fig. 2 *Flow chart of soil dry zone testing system operation*

Table 1 Tested soil samples composition used in the laboratory device testing

Sample number	Weight percentage, %				Classification
	Clay	Sand	Silt	Moisture	
1	10	87	3	3.2	fine sand and clay, grain size between 0.15 and 1.18 mm poor in silt
2	28	70	2	5	fine sand and clay, grain size between 0.15 and 1.18 mm no gravel, and poor in silt
3	39	59	2	6.1	fine sand and clay, grain size between 0.15 and 1.18 mm, no gravel, and poor in silt.
4	50	50	—	7.1	fine sand and clay, grain size between 0.15 and 1.18 mm, no gravel, and poor in silt
5	60	39	1	9	fine sand and clay, grain size between 0.15 and 1.18 mm, no gravel, and poor in silt
6	83	15	2	20	fine sand and clay, grain size between 0.15 and 1.18 mm, no gravel, and poor in silt

From this table, it is also noticed that the critical temperature falls between 50 and 58°C depending on the soil compositions and the moisture content. The critical temperature is defined as the temperature at which the dry zone started to be formed in the soil. The thermocouples are arranged as shown in Fig. 3. The distance between each thermocouple and the other is 1.5 cm.

The temperature distribution indicates that the relation between the temperature and the distance for each soil has two slopes, as given in Fig. 4 each one indicates to a zone that has different soil thermal resistivity.

The first zone given in Fig. 4 is formed near the heat source that represents the cable and this is the drying zone and the second zone which usually starts at the end of the first one and it is known as the wet zone. The purpose of this figure is to calculate the dry and wet thermal resistivity of each tested soil. Each zone thermal resistivity can be obtained by using IEC60287 [1]:

$$\sigma = \frac{(\mathrm{d}T/\mathrm{d}Z)}{Q_\mathrm{h}} \quad (4)$$

where $\mathrm{d}T/\mathrm{d}Z$ is the temperature gradient $^\circ$C/m; σ is the soil resistivity °C/m /W and Q_h is the heat flux density W/m^2.

The velocity of the dry zone formation can be calculated by using the relation:

$$\frac{Z_1 - Z_2}{t_1 - t_2} = \text{velocity of dry zone}\, Z_1 > Z_2 \quad (5)$$

where Z_1 is the position of the dry zone at any point recorded at t_1, and Z_2 is the position of the dry zone at any point recorded at t_2.

The velocity of the dry band formation for each tested soil is calculated using (4) and given in Table 3 when the heat flux

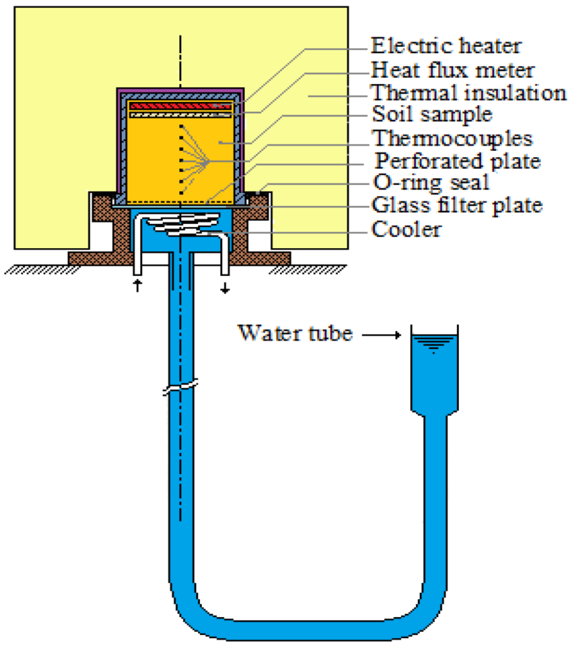

Fig. 3 *Soil testing arrangement*

Table 2 Soil samples thermal resistivity, critical temperature and time of dry zone formation

Soil sample	Soil thermal characteristics				
	Wet soil thermal resistivity	Soil thermal resistivity °C.m/W		Critical temperature and time of dry zone formation	
		At starting of the dry zone	At end of the dry zone	Critical temperature °C	Time to start dry band in hours
1	0.91	1.9	2.63	58	1.933
2	0.821	1.8	3.15	55.5	3.1
3	0.818	1.8	3.5	54	3.5
4	0.805	1.7	3.8	52	3.75
5	0.794	1.6	4.6	51	4.1
6	0.746	1. 4	1.91	50	4.5

density was 650 W/m^2. Increasing the heat flux density leads to rapid increase in dry band formation [1].

From Table 3 it is noticed that the speed of the formation of the dried layers began by slow rate and then accelerates, after that, it slows down again when approaching the state of constancy. This phenomenon is consistent with all soil types that have been tested but the values of the speed of dry zone formation differ from one soil to another. This indicates that the time of dry zone formation and consequently the device operating time changes from one soil to another.

4 Laboratory and field testing of the suggested device

4.1 Laboratory testing of the device

Laboratory experiments are done for testing the suggested monitor in determining the dry zone formation for each tested soil. The suggested device recorded dry area formation by continuous measurement of the soil temperature using temperature sensors (thermocouples) as given in Fig. 5. As shown in this figure the soil testing device that is shown in Fig. 3 is connected with the device using a group of thermocouples. The output voltages of the thermocouples in mVs represent the soil temperature are amplified by the signal amplifying circuit and compared with an external voltage (DC reference voltage) using the comparator circuit given in Fig. 1. This reference voltage represents the critical temperature level of the dry zones formation for each soil type in mVs. When the amplified thermocouple voltage reaches to be greater than the reference voltage, the monitor circuit works to give the signal to trigger the alarm device.

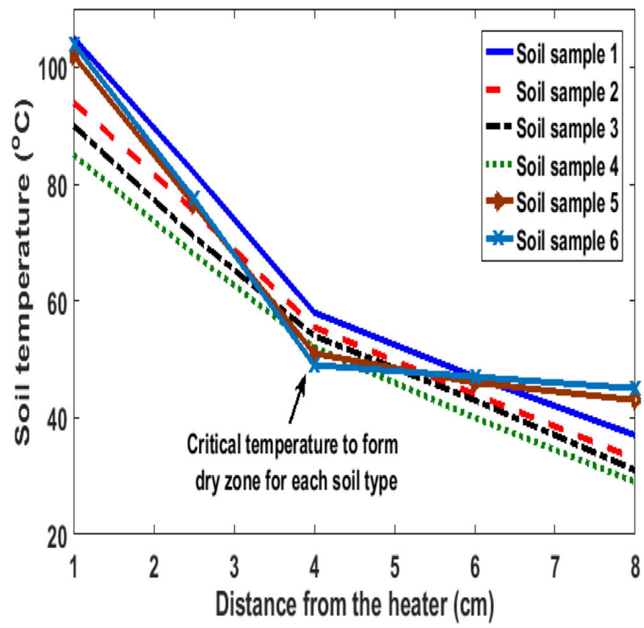

Fig. 4 *Relation between measured temperatures and the distance for the six soil samples when pf = ∞, Q_h = 650 W/m^2 after reaching to steady-state*

Several laboratory experiments are conducted to test the reliability of the proposed device. The details of the device testing, using the test arrangement of Fig. 5 is given in Table 4. The device is tested using soil samples given in Table 1. Ten tests are done

Table 3 Velocity of dry zone formation in tested soil samples

Sample number	Z	t	Velocity of dry area formation, cm/min
1	2.5	116	0.02155 between 0 and 116 min, 0.0435 between 116 and 162 min and 0.0284 between 162 and 250 min
	4.5	162	
	7	250	
2	2.5	110	0.0227 between 0 and 110 min, 0.04 between 110 and 160 min and 0.0294 between 160 and 245 min
	4.5	160	
	7	245	
3	2.5	104	0.0240 between 0 and 104 min, 0.0556 between 104 and 140 min and 0.0301 between 140 and 223 min
	4.5	140	
	7	223	
4	2.5	100	0.025 between 0 and 100 min, 0.0571 between 100 and 135 min and 0.0313 between 135 and 215 min
	4.5	135	
	7	215	
5	2.5	102	0.0204 between 0 and 102 min, 0.087 between 102 and 125 min and 0.0333 between 125 and 200 min
	4.5	125	
	7	200	
6	2.5	122	0.0204 between 0 and 122 min, 0.0392 between 122 and 173 min and 0.0258 between 173 and 270 min
	4.5	173	
	7	270	

Z is the distance between the thermocouple and the heat source in (cm).
t is the time to form dry zone and give alarm from the circuit in (min).

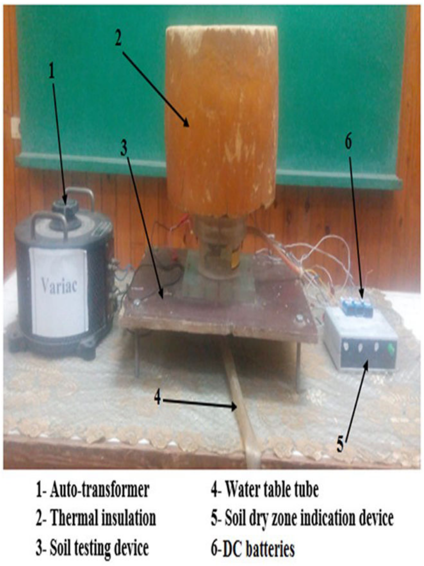

Fig. 5 *Monitor device testing arrangement*

using each sample with 2 h separation between each test and the other. Comparing the time of the device operation and the soil temperature at which the device operates given in Table 4 with the time of dry zone formation and the critical temperature shown in Table 2 it can be noticed that the device proved excellent efficiency and accuracy in determining the formation of a dried layer in the six sample soils given in Table 1.

The overall percentage of the instrument accuracy is calculated based on the total successful operation using the following formulas [28, 41]:

$$S_{Fj} = \frac{P_{Fj}}{\text{Total number of the device operation for each } F_j} \times 100 \tag{6}$$

$$C_{Fj} = \frac{\sum_{j=1}^{j=n} S_{Fj}}{n} \times 100 \tag{7}$$

where F_j is the soil sample code, S_{Fj} is the percentage successful operations of the device operation, P_{Fj} is the number of successful operations, j is the number of device operations in each site ($j = 1, 2, 3, 4, \ldots, n$), and C_{Fj} is the average of the overall percentage successful operations of all sites.

Table 4 Results of the device testing in the Laboratory

Soil samples	Time of the device operation, h	Soil temperature at the device operation, °C	Comments and number of tests
1	2	58	the test is repeated ten times, fresh soil sample is used in each test. The device succeeded to indicate to the dry zone without any fail
2	3.5	56	the test is repeated ten times, fresh soil sample is used in each test. The device succeeded to indicate to the dry zone with one fail
3	3.5	54	the test is repeated ten times, fresh soil sample is used in each test. The device succeeded to indicate to the dry zone without any fail
4	3.85	52	the test is repeated ten times, fresh soil sample is used in each test. The device succeeded to indicate to the dry zone without any fail
5	4.7	51	the test is repeated ten times, fresh soil sample is used in each test. The device succeeded to indicate to the dry zone without any fail
6	2	50	the test is repeated ten times, fresh soil sample is used in each test. The device succeeded to indicate to the dry zone without any fail

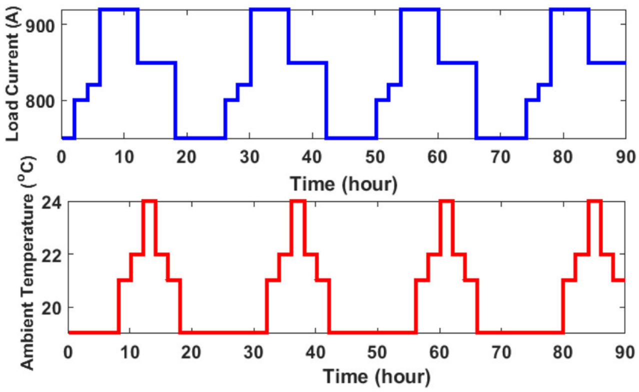

Fig. 6 *33 kV cable load cycle and the ambient temperature*

Table 5 Construction details of the monitored cable

Cable details	33 kV
Conductor material	Copper (single-core)
Conductor area, mm^2	1000
Conductor diameter, mm	40.2
Insulation type	XLPE
Insulation diameter, mm	59.5
Screen type	Aluminium
Screen diameter, mm	64
Cover type	PVC
Overall cable diameter, mm	71

Applying the above formulas to calculate the instrument accuracy indicates that the device accuracy is about 98.3% after 60 tests done on the different soil samples given in Table 1 and can be used as back-fill materials surrounding underground cables.

4.2 Field testing of the device

Field tests are done on the suggested monitor to check its reliability. The measurements are done in the field during loading the 33 kV flat formation cable by its load cycling given in Fig. 6. Table 5 gives the monitored cable construction details.

In the cable load cycle given in Fig. 6, the current reached 900 amperes in some hours through the day. The ambient temperature during the measurements was varied between 0 and 10°C during the night and 10 and 24°C during daylight hours. Five thermocouples are distributed radially on the cable path; the first thermocouple is fixed on the cable sheath and the space between each thermocouple and another one is taken as 5 mm for the remaining thermocouples.

The device is tested in selected sites along the cable route. The cable surrounding the soil of the first site contains the majority sand having grain size between 0.15 and 1.18 mm besides about 10% of clay to improve soil retention. This back-fill composition is similar to the tested soil sample 1 given in Table 1. In other places, the back-fill soil composition was 60% sand besides about 40% clay. Its components are approximately similar to the investigated soil sample 5 given in Table 1. The temperature of the soil surrounding the middle cable is calculated using IEC 60853-2 modified method. In this method, the temperature of the soil surrounding the cable is calculated according to the relation

$$\theta_e(t) = \frac{\rho_{\text{soil}} W_I}{4\pi}\left\{\left[-Ei\left(\frac{-D_e^2}{16t\delta}\right) - \left[-Ei\left(\frac{-L^2}{t\delta}\right)\right]\right] + \sum_{K=1}^{K=N-1}\left[-Ei\left(\frac{-(d_{pk})^2}{4t\delta}\right) - \left[-Ei\left(\frac{(d'_{pk})^2}{4t\delta}\right)\right]\right]\right\} \tag{8}$$

The dynamic temperature of the soil surrounding the centre cable (θ_e) can be determined by using (8) [21, 38]. Where $-Ei(-x)$ is the exponential integral, δ is the thermal diffusivity of the soil, W_I is the cable total power losses calculated according to the IEC 60287-1-3 [1]. d_{pk} and d'_{pk} are the distances from the centre of cable (k) to the centre of cable (p) and distance from the image of the centre of cable (k) to the centre of cable (p), respectively, and N is cable number.

The general thermal resistivity ρ_{soil} of the back-fill surrounding soil of the cable changes with soil temperature, soil moisture content and its dry density as reported by Groeneveld *et al*. [38]:

$$\log_{10}\rho_{\text{soil}} = (g_1 - g_2\gamma_d)x_1(\theta) + \frac{g_3}{g_4 + (G_1/x_2(\theta))} \tag{9}$$

where

$$x_1(\theta) = 1 + \frac{g_5(\theta - \theta_\text{a})}{(\gamma_\text{d} - \gamma_\text{min})} + g_6(\gamma_\text{max} - \gamma_\text{d})(\theta - \theta_\text{a})^2$$

$$x_2(\theta) = (1 - g_7(\theta - \theta_\text{a}))\frac{\gamma_\text{d}}{\gamma_\text{w}}$$

In the above equation, γ_max, γ_min and γ_d are the maximum, minimum and dry density of the soil, respectively, θ_a and θ are the ambient and soil temperature, respectively, and the values of g_1 to g_7 are given as follows [38]:

$$g_1 = 1.35,\quad g_3 = 0.017,\quad g_5 = 0.299,\quad g_7 = 0.01$$
$$g_2 = 1.15\times 10^{-3},\quad g_4 = 0.0179,\quad g_6 = 1.08\times 10^{-7}$$

The determination of the specific heat at each moisture content amount is done according to the relation given in [19, 20]:

$$C_\text{psoil} = C_\text{d}\gamma_\text{d} + C_\text{w}\gamma_\text{w}G_1 \tag{10}$$

where C_psoil is the soil specific heat in (J/m^3.°C), C_d is the dry specific heat in (J/Kg.°C), C_w is specific heat of water in (J/Kg.°C), γ_d is dry density of the tested soil, γ_w is water density and G_1 is the soil moisture content. To include the probability of dry zone formation in the back-fill soil around the cable during load cycling, the variations of the soil resistivity and its volumetric specific heat are inserted into the designed program used in the calculations of

Table 6 Soil parameters surrounding the monitored cable

Soil samples	Site soil moisture content G_1	Maximum, minimum and dry density, Kg/m^3 γ_{max}	γ_{min}	γ_d	Specific heat, J/Kg.°C Wet	Dry
first site (A)	0.035	1651	1450	1600	965	900
second site (B)	0.075	1585	1250	1480	970	835

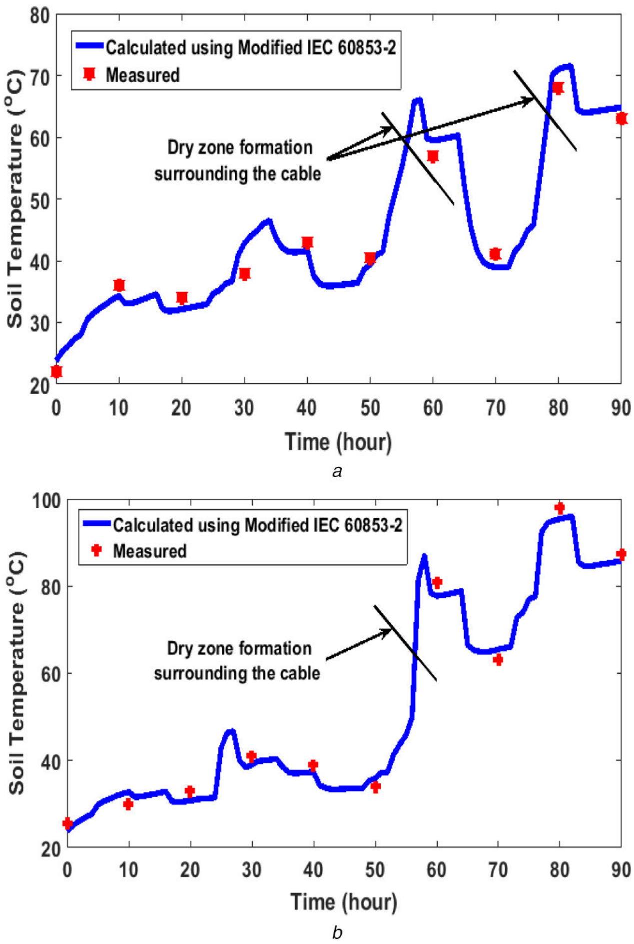

Fig. 7 *Soil surrounding the cable temperature using modified IEC 60853-2 method and field measurements*
(a) First site (A),
(b) Second site (B)

Table 7 Results of the device testing at the two sites

Test site	Time to start the dry zone, h	Soil temperature at the device operation, °C	Comments	Number of tests
(A)	55	58	dry zone is formed after 55 and stayed to about 10 h and started again after 78 h of loading and stayed for 12 h	instrument is tested for 50 times and failed to give alarm in two times because of one of sensors failure
(B)	53	51	dry zone is formed after 53 h of loading for 37 h	instrument is tested for 100 times and failed to give alarm in one time because wrong adjustment of comparator circuit

the dynamic temperature distribution of the cable surrounding soil during dynamic loading according to the modified IEC 60853-2. The soil parameters surrounding the monitored cable are given in Table 6.

Fig. 6 gives the cable load cycle and ambient temperature through 4 days. The cable details and the load cycle are reported by the Egyptian Electrical Grid Company [39, 42]. Fig. 7 shows the calculated and measured soil temperatures around the middle cable of the cable system. The test is repeated along the cable path.

More than 150 tests are conducted on the 33 kV in two sites (A) and (B). The device failed to give an alarm when reaching to the dry zone formation around the cable two times from 50 tests done in site (A), as shown in Table 7 the cause was one of the sensors has failed. In site (B) about 100 tests are carried out with one time fail because of the wrong adjustment of the comparator circuit. It is necessary to reduce the cable loading when the dry zone is formed around the cable, by the separation of un-effective loads to decrease the heat produced by the cable and then reduce the temperature of the soil as well. Table 7 gives the details of the device testing at two sites.

The overall percentage consistency of the instrument 150 tests done in the field is calculated based on the total successful operations using the formulas of (6) and (7) [41]:

In this case:

F_j: soil site code A or B;

S_{Fj}: the percentage successful operations of the device at the site;

P_{Fj}: number of successful operations;

j: number of device operations in each site ($j = 1, 2, 3, 4, \ldots, n$);

C_{Fj}: the average of the overall percentage successful operations of all sites.

By calculating the accuracy of the device in the field using the above data given in Table 7 it is found to be 98.5%. The device has demonstrated high accuracy in the definition of the dry zone around the cable route at the site.

5 Discussion

The strategies of underground power cables monitoring are sophisticated based on different devices and many of them are costly. As an example, conventional methods of cable monitoring using XLPE, PVC, EPR and other power cables insulating materials thermal endurance characterisations are based on analytical methods [39, 40]. In some techniques, the cable temperature can be visualised on the screen or shown as a profile [43, 44]. These diagnosis techniques are either too time-consuming or some can give mysterious data that cannot be interpreted. Software systems of the cable temperatures can be recorded by using a set of elements, which are installed at hot spots of the power cable route [39]. Another technique for measuring the surrounding cable soil drying time is extrapolated by probe, it can be used to create operational conditions that will reduce the probability that soil will become thermally unstable. Other underground power cable monitors are designed to be based on cable historical operation temperature, while others are designed based on procedure to estimate the degree of ageing for an underground power cable considering thermal stresses. The disadvantage of such these monitors is that they need different parameters related to thermal ageing and thermal lifetime estimation.

This paper suggested a new on-line device for underground power cable monitoring based on recording the temperature of the soil surrounding the cable. The advantages of the proposed technique, when compared with the above conventional methods, can be summarised as follows:

(i) The device costs very little compared to any other systems, its cost is no more than several tens of dollars.
(ii) There is no direct connection between the device sensors and the cables as the soil temperature is monitored around the cable, and does not expose during its operation to the cable voltage or current effects. This means that it is safe.
(iii) It is an on-line monitor, so it is not time consuming.
(iv) The device accuracy reached to about 98.3% after 60 tests done in the laboratory and the field accuracy reached 98.5% after about 150 tests carried out in the field.
(v) The device has simplicity in the design.

One of the limitations of the proposed device is that the reference voltage has to be calibrated and adjusted for each back-fill soil. This needs to measure the critical temperature of the soil surrounding the cable every time before installing the device.

6 Conclusions

In this paper, monitor for dry zone formation in the back-fill surrounding soil of the underground power cables is suggested. It has been tested in the laboratory using different types of soil with different moisture rates. In the tested soil, the amounts of sand and clay are changed to cover the soil that can be used as back-fill material. The monitor is tested in the field to check its accuracy. The device demonstrated excellent efficiency and accuracy in determining the formation of a dried layer in the soil. Its accuracy reached to about 98.3% after 60 tests done in the laboratory and the field accuracy reached to 98.5% after about 150 tests carried out in the field. It is simple, cheap and not time consuming. One of the device limitations is the need for reference voltage adjustment for each soil type and measuring of the critical temperature at which dry zone is formed can be considered as another limitation.

7 References

[1] IEC publication 60287-1-3: 'Calculations of the continuous current rating of cables (100% load factor)', 1982
[2] Dorison, E., Anders, G.J., Lesur, F.: 'Ampacity calculations for deeply installed cables', *IEEE Trans. Power Deliv.*, 2010, **25**, (2), pp. 524–533
[3] de Leon, F.: 'Major factors affecting cable ampacity'. presented at the IEEE/Power Engineering Society General Meeting, Montreal, QC, Canada, 18–22 June 2006, paper 06GM0041
[4] Anders, G.J.: '*Rating of electric power cables: ampacity computations for transmission, distribution, and industrial applications*' (IEEE Press/McGraw Hill, Seattle, WA, USA, 1997)
[5] Gouda, O.E., El Dein, A.Z.: 'Improving underground power distribution capacity using artificial backfill materials', *IET Gener. Transm. Distrib.*, 2015, **9**, (15), pp. 2180–2187
[6] Gouda, O.E., Osman, G.F.A., Salem, W.A.A., *et al.*: 'Load cycling of underground distribution cables including thermal soil resistivity variation with soil temperature and moisture content', *IET Gener. Transm. Distrib.*, 2018, **12**, (18), pp. 4125–4133
[7] Gouda, O.E.: 'Formation of the dried out zone around underground cables loaded by peak loadings', *Model. Simul. Control*, 1986, **7**, (3), pp. 35–46
[8] Gouda, O.E., Osman, G.F.A., Salem, W.A.A., *et al.*: 'Cyclic loading of underground cables including the variations of backfill soil thermal resistivity and specific heat with temperature variation', *IEEE Trans. Power Deliv.*, 2018, **33**, (6), pp. 3122–3129
[9] Gouda, O.E., Amer, G.M., El Dein, A.Z.: 'Improving the under-ground cables ampacity by using artificial backfill materials'. Proc. of the 14th Int. Middle East Power Systems Conf. (MEPCON'10), Cairo University, Egypt, 19–21 December 2010, pp. 38–43
[10] Al-Saud, M.S., El-Kady, M.A., Findlay, R.D.: 'Combined simulation-experimental approach to power cable thermal loading assessment', *IET Gener. Transm. Distrib.*, 2008, **2**, (1), pp. 13–21
[11] Ocłoń, P., Cisek, P., Pilarczyk, M., *et al.*: 'Numerical simulation of heat dissipation processes in underground power cable system situated in thermal backfill and buried in a multilayered soil', *Energy Convers. Manage.*, 2015, **95**, pp. 352–370
[12] Al-Saud, M.S., El-Kady, M.A., Findlay, R.D.: 'A new approach to underground cable performance assessment', *Electr. Power Syst. Res.*, 2008, **78**, pp. 907–918
[13] de León, F., Anders, G.J.: 'Effects of backfilling on cable ampacity analyzed with the finite element method', *IEEE Trans. Power Deliv.*, 2008, **23**, (2), pp. 537–543
[14] Hegyi, J., Klestoff, A.: 'Current-carrying capability for industrial underground cable installations', *IEEE Trans. Ind. Appl.*, 1988, **24**, (1), pp. 99–105
[15] Hanna, M.A., Chikhani, A.Y., Salama, M.M.A.: 'Thermal analysis of power cables in multi-layered soil. Part 3: case of two cables in a trench', *IEEE Trans. Power Deliv.*, 1994, **9**, (1), pp. 572–578
[16] Yenchek, M.R., Cole, G.P.: 'Thermal modelling of portable power cables', *IEEE Trans. Ind. Appl.*, 1997, **33**, (1), pp. 72–79
[17] Anders, G.J., Chaaban, M., Bedard, N., *et al.*: 'New approach to ampacity evaluation of cables in ducts using finite element technique', *IEEE Trans. Power Deliv.*, 1987, **2**, (4), pp. 969–975
[18] El-Kady, M.A.: 'Calculation of the sensitivity of power cable ampacity to variations of design and environmental parameters', *IEEE Trans. Power Appar. Syst.*, 1984, **PAS-103**, (8), pp. 2043–2050
[19] Kellow, M.A.: 'A numerical procedure for the calculation of the temperature rise and ampacity of underground cables', *IEEE Trans. Power Appar. Syst.*, 1981, **PAS-100**, (7), pp. 3322–3330
[20] Olsen, R., Anders, G.J., Holboell, J., *et al.*: 'Modelling of dynamic transmission cable temperature considering soil specific heat, thermal resistivity and precipitation', *IEEE Trans. Power Deliv.*, 2013, **28**, (3), pp. 1909–1917
[21] IEC Standard 60853-2: 'Calculation of the cyclic and emergency current ratings of cables, part 2: cyclic rating factor of cables greater than 18/30 (36) kV and emergency ratings for cables of all voltages', Publication 853-862, 1989
[22] Olsen, R.S., Holboell, J., Gudmundsdóttir, U.S.: 'Dynamic temperature estimation and real time emergency rating of transmission cables'. presented at the IEEE Power Energy Society General Meeting, San Diego, CA, July 2012, pp. 1–8
[23] Freitas, D.S., Prata, A.T., de Lima, A.J.: 'Thermal performance of underground power cables with constant and cyclic currents in presence of moisture migration in the surrounding soil', *IEEE Trans. Power Deliv.*, 1996, **11**, (3), pp. 1159–1170
[24] Maximov, S., Venegas, V., Guardado, J.L., *et al.*: 'Analysis of underground cable ampacity considering non-uniform soil temperature distributions', *Electr. Power Syst. Res.*, 2016, **132**, pp. 22–29
[25] Zarchi, D.A., Vahidi, B.: 'Optimal placement of underground cables to maximise total ampacity considering cable lifetime', *IET Gener. Transm. Distrib.*, 2016, **10**, (1), pp. 263–269
[26] Carlos, G., Antonio, F.O., José, C.: 'Theoretical model to calculate steady-state and transient ampacity and temperature in buried cables', *IEEE Trans. Power Deliv.*, 2003, **18**, (3), pp. 667–678
[27] Anders, G.J., El-Kady, M.A.: 'Transient ratings of buried power cables part 1: historical perspective and mathematical model', *IEEE Trans. Power Deliv.*, 1992, **7**, (4), pp. 1724–1734
[28] Campbell, G.S., Calissendorff, C., Williams, J.H.: 'Probe for measuring soil specific heat using a heat-pulse method', *Soil Sci. Soc. Am. J.*, 1991, **55**, (1), pp. 291–293
[29] Koopmans, G., Gouda, O.E.: 'Transport of heat and moisture in soils with hysteretic moisture potential'. Proc. of the Fourth Int. Conf., Swansea, UK, 15–18 July 1985, vol. 2, pp. 846–874
[30] Anders, G.J., Radhakrishna, H.S.: 'Power cable thermal analysis with consideration of heat and moisture transfer in the soil', *IEEE Trans. Power Deliv.*, 1988, **3**, (4), pp. 1280–1288
[31] Donazzi, F., Occhini, E., Seppi, A.: 'Soil thermal and hydrological characteristics in designing underground cables', *Proc. Inst. Electr. Eng.*, 1979, **126**, (6), pp. 506–516
[32] Philip, J.R., De Vries, D.A.: 'Moisture movement in porous materials under temperature gradients', *Trans. Am. Geophys. Union*, 1957, **38**, (2), pp. 222–232
[33] Gouda, O.E., Abdel-Aziz, A.M., Refaie, R.A., *et al.*: 'Experimental study for drying-out of soil around underground power cables', *JKAU Eng. Sci.*, 1997, **9**, pp. 23–40
[34] Gouda, O.E.: 'Environmental impacts on underground power distribution', *Advances in Computer and Electrical Engineering* (IGI Global, Hershey, PA, USA, 2016)
[35] Gouda, O.E., Amer, G.M., El Dein, A.Z.: 'Effect of the formation of the dry zone around underground power cables on their ratings', *IEEE Trans. Power Deliv.*, 2010, **26**, (2), pp. 972–978
[36] Abu-Hamdeh, N.H.: 'Thermal properties of soils as affected by density and water content', *Biosystems Eng.*, 2003, **86**, (1), pp. 97–102
[37] Bristow, K.L., Campbell, G.S., Calissendorff, K.: 'Test of a heat-pulse probe for measuring changes in soil water content', *Soil Sci. Soc. Am. J.*, 1993, **57**, (4), pp. 930–934
[38] Groeneveld, G.J., Snijders, A.L., Koopmans, G., *et al.*: 'Improved method to calculate the critical conditions for drying out sandy soils around power cables', *IEE Proc. C, Gener. Transm. Distrib.*, 1984, **131**, (2), pp. 42–53
[39] Popovac-Damljanovic, A., Sredojevic, M., Nikolajevic, S., *et al.*: 'Thermal monitoring of high voltage cables', F-75008 Paris, B1-210, 2006
[40] Singh, K.: 'Cable monitoring solution'. PhD, B.A MEng (UK), MIEEE, UK, November 2011, Cabos 11, Maceio. Available at http://www.jicable.org/Other_Events/cabos11/Slides/Cabos_5.1.pdf
[41] Muhamad, N.A., Phung, B.T., Blackburn, T.R., *et al.*: 'Comparative study and analysis of DGA methods for transformer mineral oil'. IEEE Lausanne Power Tech, University of New South Wales, Sydney, Australia, 2007, pp. 45–50
[42] Egyptian Electricity Distribution Companies (EEDC) Reports, 1991–2016
[43] Marmon sensing solutions: 'Power cable monitoring', 2019. Available at https://www.marmonsensing.com/Applications/Power-Cable-Monitoring
[44] Bandweaver: 'Distributed sensing technology for power cable monitoring system', 2019. Available at https://www.bandweaver.com/sectors/power/power-cable-monitoring